International Journal of Chemical and Biochemical Sciences
(ISSN 2226-9614)

Journal Home page:www.iscientific.org/Journal.html

Decolorization of Cotton Waste by Photocatalytic Degradation

G.Padma Priya[1], Deepak Sharma[2], Nirjara Singhvi[3]*

[1]*Department of Chemistry and Biochemistry, School of Sciences, Jain University, Bangalore, India.*

[2]*School of Agriculture Sciences, Jaipur National University, Jaipur, India.*

[3]*School of Allied Science, Dev Bhoomi Uttarakhand University, Dehradun, Uttarakhand, India.*

Abstract

Dyeing is a common practice in many sectors, including textiles, to color things. Even in extremely small concentrations, such dyes are observable and should not be present in water. The photocatalyst approach has a decent chance of removing color in the wastewater. In the current study, $g - C_3N_4$ was produced by the heat degradation of mylamine, was described, and then used to remove ethylene blue (EB) and methyl orange (MEO). The equilibrium data for the photo-degradation of EB are determined preparation stage for the pH 7, photo-degradation of MEO is reported to need 0.04 g/L of catalyst. as opposed to 0.08 g/L at a coagulant pH 9. Consequently controlling parameters, like adsorbent, the concentration of dye, and pH, have been researched, and the findings show that. The study of the kinetics of heterogeneous photocatalysis responses revealed that the response followed pseudo-first-order kinetics as well as that the Langmuir-Hinshelwood design adequately represented it. The adsorption equilibrium value for Langmuir-Hinshelwood and the kinetics level variable for EB have been discovered to be k = 0.7756 ($mg/L.min$) and 0.0184 L/mg, correspondingly. The adsorption equilibrium constant and surface reaction rate constant for MEO have been discovered to be 10.537 ($mg/L.min$) and 0.004L/mg, correspondingly.

Keywords: Dyeing, ethylene blue (EB), methyl orange (MEO), photo-degradation

Full length article **Corresponding Author,* e-mail:g.padmapriya@jainuniversity.ac.in

1. Introduction

The textile industry uses a lot of chemicals and water, and it also produces a lot of wastewater in the form of colorful dye effluents. Colored effluents are harmful to nature and harm the ecology and environment. 200-400 gallons of water were used by the textile industry to produce 1 kg of cotton [1]. Methylene blue's photocatalytic dye removal was estimated utilizing a photochemical reactor with $wo_3$and sno_2 photocatalysts in the presence of UV light.Photocatalytic substances based on sio_2, nitrogen-doped Tio_2 micro, and various HY zeolite concentrations (0, 12, 25, and 50%). During photocatalytic processes, it typically investigates the redox processes that start close to the electronic surface upon exposure to laser illumination to degrade pollution [2].The finishing and dyeing procedures used in the textile industry use a lot of water and produce a lot of pollution as a result. Due to the large concentrations of organic and inorganic substances that are chemically or biologically resistant that they contain, textile effluents are hazardous to the environment and the general people if they are not adequately handled. Highly colored effluent from the textile sector distinguishes it [3].At even low concentrations [4], these dyes are prominent and should not be present in water. The photocatalytic method has a decent chance of removing color from wastewater. Ethylene blue (EB) and methyl orange (MEO) were removed using $g - C_3N_4$which was produced in the current study by the thermal breakdown of mylamine.

Marine organisms and health impacts are both negatively impacted by the wide array of colors and chemicals found in textile effluents. Consequently, before emissions, adequate treatment is required. One of the best methods for treating wastewater contaminated with organic pollutants is photocatalysis [5]. Most photocatalysts are made of metal oxides, likeTio_2, Wo_3, Zn_o, Sno_2, BiV_{O4}, $Bi2O_3$, andZ_{rO_2}. The objective of modern developments in photocatalysis is to find adequate niche applications for new semiconductor materials [6]. Titanium dioxide is the photocatalyst that has been recognized the most and is used to treat water and split water. Even though Ag, Tio_2, and biochar work together, it was found that all catalysts that had Ag added had better photocatalytic degradation performance than just Tio_2[7]. The highest decolorization and mineralization efficiencies were 97.48% and 85.38 %, respectively. It is necessary to treat the industrial wastewater that comes from the chemical treatments used in the textile industry. Organic dyes in wastewater from textiles are thought to be one of the most harmful things to the environment. These organic dyes are dangerous, don't change over time, and are not compostable [8].

The literature on heterogeneous photocatalysis has documented several publications, which typically

investigate the redox processes that start close to the surface of semiconductors after being exposed to light irradiation to degrade pollutants [9]. $CZnO$-dots were customized using a one-step microwave pyrolysis technique, which was similar to an earlier, but slightly modified, approach [10]. In a summary, 30 ml of DDW was used to dissolve 3g of gum ghatti powder. The mixture was then stirred until it became transparent. The resulting mixture was then combined with zinc acetate, which was added in weight percent of 0.5, 1, 1.5, and 2 of the gum extract, and agitated for 30 minutes. It is then placed for 20 minutes in a microwave oven that is set to 80% power. The mixture was acquired in the raw form, aerated at room temperature, and then agitated for 30 minutes at around 9000 rpm.The proposed method of MG dye photocatalytic degradation using visible-light response$CZnO$-dots is schematically illustrated under the trapping investigations. ZnO Serves as the e- donor and produces the e- during the photocatalytic reaction by absorbing light. The CB of the C-dots receives the stimulated [11]. As pH has a considerable impact on photocatalytic decolorization and is consistent with the evidence of surface charge characteristics of nanocatalysts, pH is an important criterion.

The combination H_{2O_2}-assisted photocatalytic approach that has been suggested is very effective at reducing the dye content but less effective at eliminating COD from wastewater [12]. For the residual COD in the wastewater to completely mineralize, extra treatment is therefore needed. To comprehend the function of H_2O_2, Tio_2, and MC in dye decolorization, the synergism of the suggested photocatalytic degradation was examined. The coupled hydrogen peroxide-aided photocatalytic degradation of MB dye was matched to the degradation rate constant of each separate treatment method. One possible proposed process for the RhB photocatalytic degradation facilitated by cotton textiles covered with synthetic nanocomposites [13].The photocatalysts produce electron-hole pairs when exposed to UV and visible light.Holes may be transmitted to water molecules, resulting in the production of hydroxyl radicals.

According to this study [14], nanoparticles were more effective against gram-positive bugs than gram-negative bacteria. This occurred because gram-negative bugs often possess an additional outer coat of lipopolysaccharide and peptidoglycan that aids them in minimizing any potential harm from nanoparticles. The degradation of the contaminated wastewater by solar photocatalytic means was examined in this study. As a photocatalyst, Tio_2 Evonik Aeroxide P25 was utilized. Tio_2has to be immobilized into one of the readily accessible polymeric substrates to make it easier to use the photocatalyst within the DIY CPC prototype. The use of polymeric waste released from textile industries as catalytic support had previously been proposed for a study [15]. In comparison to other traditional treatment procedures, the advantages primarily include the avoidance of enormous volumes of solid waste and the decrease of actual impact.

The photocatalytic reaction happens in several steps on the surface of a semiconductor, and many scientists have come up with a possible explanation for how the process works.

2. Materials and methods

2.1Synthesis of $g-C_3N_4$

All of the chemical compounds used in the synthesis and analysis were available on the market and did not need to be treated in any way before they were used. Melamine was used to make the graphitic C_3N_4 powder through a process called polycondensation at high temperatures. Usually, a beaker with a rubber stopper and 5g of melamine was arranged in it and heated in a fume hood at 500°C for 4 hours at the same percentage of 20 degrees Celsius every minute. The yellow substance that was extracted was afterward dried and pulverized for use in the future.

2.2 Making of methyl orange stock solution

For soaking 1g of ethylene blue (eb) in 1 liter of distilled water, a 1000 ppm stock solution of methyl orange is created. The serial dilution is then used to create 4 alternatives with ratios of 75, 100, 150, and 200 parts per million (ppm) were the corresponding values.

2.3H_6N_6's photocatalytic efficiency

The photocatalytic activity of C_3N_4 for the reduction of methyl orange was evaluated in a 250 mL Borosilicate reaction vessel. As shown in Fig.1, 0.01g of C_3N_4 was diluted in a methyl orange reaction mixture before being added to a 1500 mL beaker of cooling water. Using a 300 W U-V light with a photons limit filter, methyl orange was photodegraded (256 nm). The UV-visible spectrophotometer was utilized for determining the concentration of methyl orange at intervals of one hour.

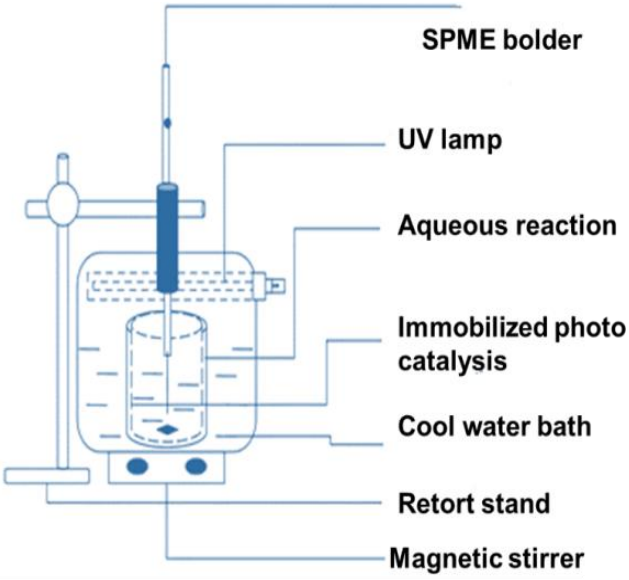

Figure 1: Instrument layout

3. Results and Discussions

3.1Analysis of $g - C_3N_4$

3.1.1FTIR evaluation

By using FTIR spectroscopy, the surface functional groups, and structure were investigated. In the range of 500 and 4000 cm1, the synthesized$-C_3N_4$'s FTIR spectra were captured using the FTIR- 8400 S Shimadzu. All three zones may be seen in the spectra at 3172 cm-1, 808 cm-1, and 1242 to 1638 cm-1. The lobes at 808 cm -1 are well known to correspond to the characteristic breathing pattern of heterocyclic layers. The bending methods of CN hetero cyclic can be observed in several prominent bands in the 1242–1638 cm–1 range. Also, it may be assumed that the strong peak at 1683 cm-1 is a sign of excellent crystallinity for$g - C_{3N_4}$. The C(sp2) -N (1320 cm-1) and C(sp2) =N (1610 cm-1) spreading patterns in a material resembling graphene are responsible for both absorbed lines, separately at a range from 1300 to 1412 cm-1 and from 1529 to 1638 cm-1 (Any such spectrum is prohibited in the FTIR spectra of pure carbon black composites).Moreover, NH stretching vibration modes are indicated by a wide band at about 3172 cm -1. As has been observed, the remaining hydrogen atoms form C-NH2 and 2 C-NH bonds that connect to the margins of the C-N sheet that resembles graphite.

3.1.2. SEM evaluation

To analyze raw data structure, scanning electron microscopy (SEM) was performed to figure out the structural sight of the produced$-C_3N_4$. In the current study, the prepared $g - C_3N_4$ was examined by SEM (JEOL JSM 6360LA). The particles in the samples had the appearance of being aggregated, and they comprised several smaller crystals as well as well-crystallized C_3N_4 nanostructures with distinct hexagonal shapes and sizes between 50 and 500 nm.

3.1.3. Time of contact's significance

It illuminates the photocatalytic functions of $g - C_3N_4$ samples with various percentages of MEO and EB, respectively, when exposed to visible light. In the presence of$g - C_3N_4$, MEO and EB levels declined very gradually under visible light. The absorbance decreased noticeably as the exposure period rose; after 1 hour of exposure to 0.04g/l of $g - C_3N_4$, almost 100% of MEO had undergone photodegradation, whereas 70% of EB had undergone the same treatment. Also, it was observed that the clearance percentage decreased as both dye concentrations were increased. The photocatalytic activity of $g - C_3N_4$ samples at varied MEO and EB concentrations, when exposed to visible light is shown in Figures 2 and 3, Table 1, and Table 2, respectively.

3.1.4. Catalyst dosage effects

Tables 3 and 4, and Figures 4 and 5 present the findings of this study on the impact of $g - C_3N_4$dose based on the elimination of MEO, accordingly. 60 minutes of the studies were conducted utilizing a 75 ppm MEO, but the EB chemical response only has 10 ppm. This can be explained by the increased opacity of the suspension that is said to result from the addition of greater amounts of $g - C_3N_4$ [25, 26]. At 0.08 g/l of$g - C_3N_4$, the highest efficient breakdown of MO was seen.

3.1.5. Initial Dye Concentration's Influence

The elimination Rate at a catalyst dose of 0.04 g/l gC3N4 for one hour is depicted in Fig. 6 and Table 5 concerning the starting decolorization intensity (MEO and EB, respectively) approaches. The impact of the starting dye concentrations (MEO and EB, respectively) in the catalyst dose of 0.04 g/l gC_3N_4 for 1 hour on the elimination percent. As anticipated, when the initial MEO and EB concentration increase, the rate of dye deterioration slows. The explanation for this is that when the initial dye concentration rises, on the interface of$g - C_3N_4$, dye particles attach in increasing numbers. Large levels of dye that has been adsorbed prevent any direct interaction with hydroxyl radicals or holes, which may have an inhibitory effect on dye breakdown. UV screening of the dye may also explain these results. High dye concentrations absorb most UV. OH• and OH2• concentrations drop, reducing catalytic reaction efficiency. Degradation of mother dye molecules may produce by-products. At initial MEO and EB levels, the terms of percentage removal drop quickly; as the original concentration rises, it falls more gradually.

3.1.6. PH effects in solutions

The MEO'sphotodegradation in the existence ofC_3N_4 was impacted by pH, but the photodegradation of EB was not, indicating that the pH has a significant impact on the photodegradation efficiency of MEO solution. At a pH of 7.0, MO was removed at the maximum rate. Nevertheless, the elimination percentage for the photodegradation of EB solution increased from a lower to a higher value. The proportion of EB removed in very acidic conditions was 30%, whereas, at higher pH levels, the removal trend climbed to 70%.

3.1.7. The kinetics of removal

Heterogeneous photocatalysis reactions are challenging processes as a result of the influence of several components and their interactions. The rate equation may be expressed as follows using the measured rate constant (k_{obs})

$$-r_{phenol} = -\frac{dC_{phenol}}{dt} = k_{obs}C_{phenol} \quad (1)$$

The kinetic model of the fictitious first order ($n = 1$) submit equation 1 in the format shown below

$$-In\left(\frac{C_{phenol}}{C_{phenol\ 0}}\right) = k_{obs}t \quad (2)$$

Give the following equations in the linear example for the pseudo-second-order kinetics model ($n = 2$)

$$\frac{1}{C_{dye}} - \frac{1}{C_{dye0}} = k_{obs}\ t \quad (3)$$

$$r = \frac{dC_{phenol}}{dt} = \frac{kK_{phenol}\ [C_{phenol}]}{1+K_{phenol}\ [C_{phenol}]} \quad (4)$$

$$\frac{1}{k_{obs}} = \frac{1}{kK_{phenol}} + \frac{C_{phenol0}}{k} \quad (5)$$

Table 1: Removal of MEO

Catalyst Dosage (g/l)	**Removal %**
0	0
0.05	75
0.1	90
0.15	95

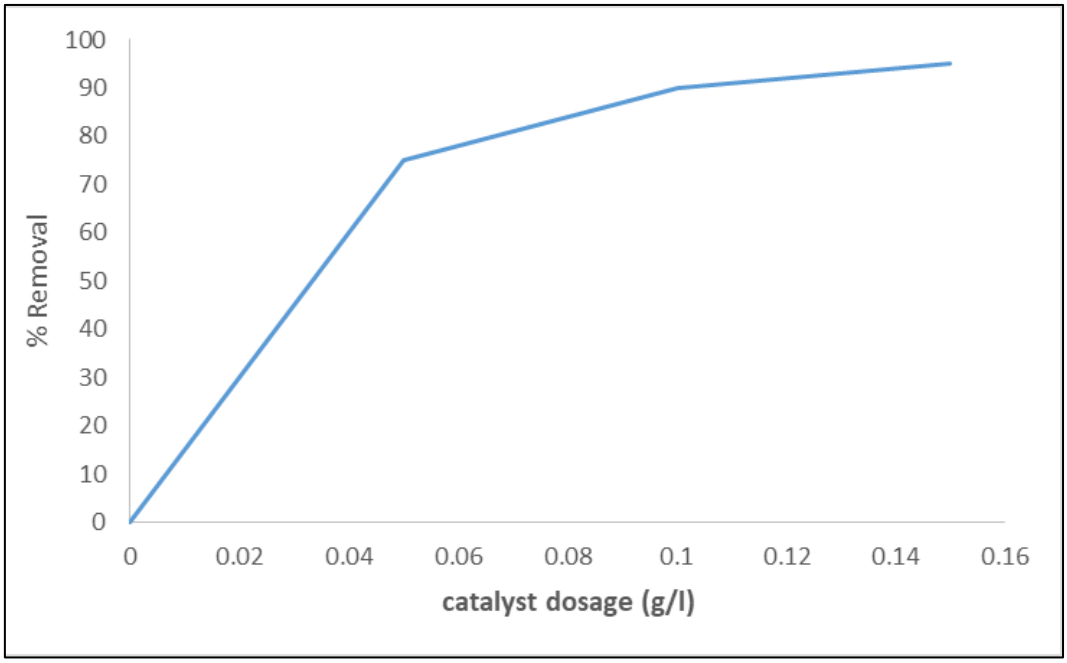

Figure 2: Removal of MEO under visible light irradiation using $g-C_3N_4$(0.04 g/l of$g-C_3N_4$).

Table 2: Removal of EB

Time (min)	**% Removal**	
	0.04 $g-C_3N_4$	**0.08 $g-C_3N_4$**
0	0	0
20	40	60
40	50	60
60	70	75

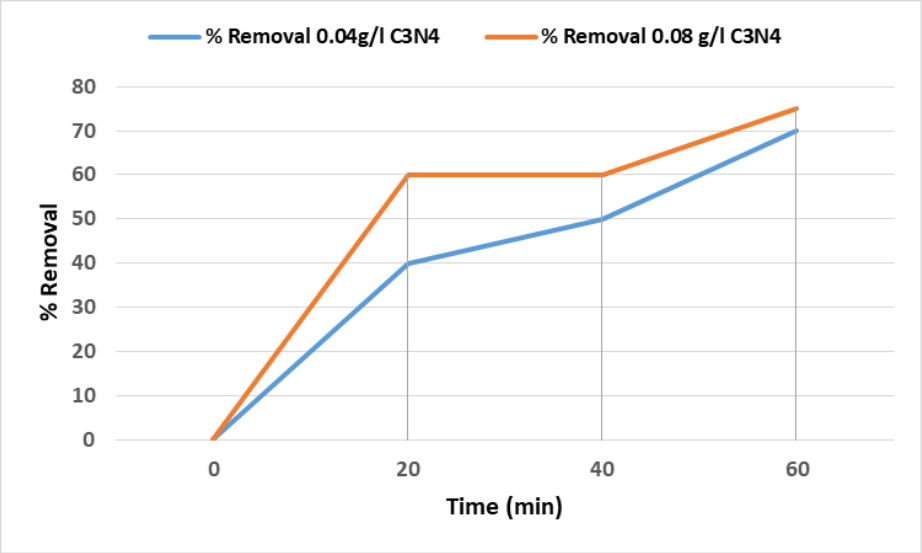

Figure 3: Visible light-induced EB elimination of$g-C_3N_4$ (0.04 g/l of $g-C_3N_4$)

Table 3: Dose and MEO elimination

The concentration of dye (ppm)	**Removal %**
50	100
100	85
150	83
200	80

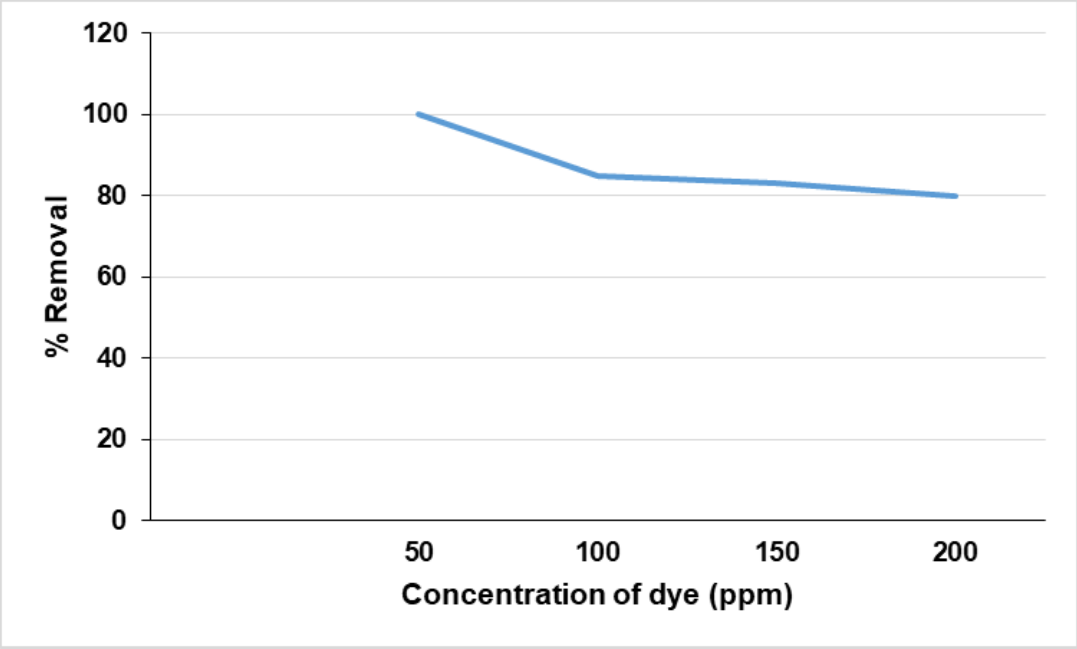

Figure 4: $g-C_3N_4$doseand MEO elimination 100 ppm coloring dilution for 1 hr.

Table 4: Removal of EB (second order)

Dye Concentration (ppm)	% Removal
10	70
20	55
30	60
40	10

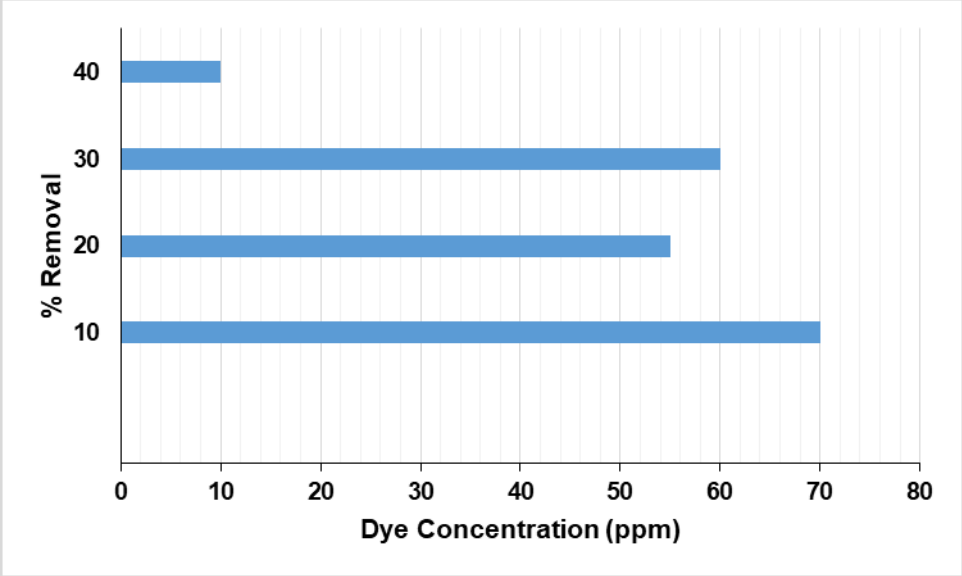

Figure 5: EB elimination via $g - C_3N_4$ dose 10 ppm dye solution for 60 min.

Table 5: pH and MO reduction

pH	% Removal
5	30
10	90
15	50

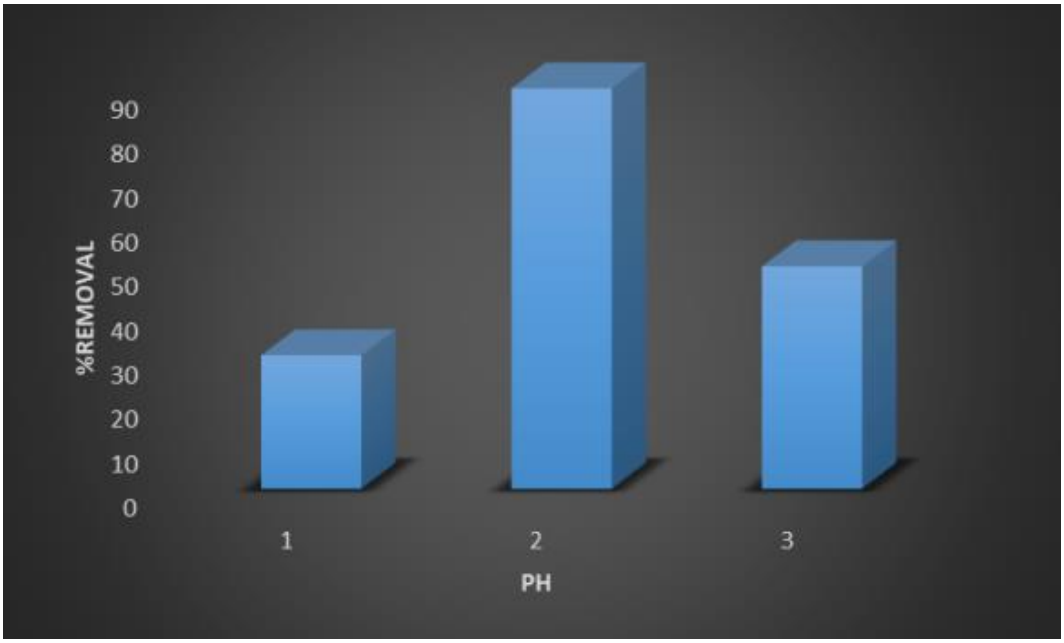

Figure 6: pH and MO reduction for Conc. 100 ppm (0.04 g/l of $g - C_3N_4$ for 1hr)

In equations (4) and (5), $Cdye0$ denotes the starting dye concentration (ppm), $Kdye$ denotes the rate constant value according to the Langmuir-Hinshelwood model (L/mg), k denotes the surface reaction's rate constant ($mg/L.min$), and $kobs$ is the pseudo-first-order rate parameter. k = 10.537 ($mg/L.min$) is the integral gain for the MEO contact reactivity, as well as the optimum factor for binding MEO, is $Kdye = 0.004\ L/mg$, as shown by Eq.(5), which states that 1/kobs against [Cdye0] is a straight line. The calculated rate of regression R is 0.9807, which indicates that the Langmuir-Hinshelwood kinetic model matches the photodegradation of MO catalyzed by$g - C_{3N_4}$.

The rate expression for MEO degradation by photocatalysis utilising $g - C_{3N_4}$ is

$$r = \frac{0.0382*[C_{dyw}]}{1+0.004*[C_{dye}]} \qquad (6)$$

An expression for the rate equation of the chemical interaction of EB is k = 0.7756 ($mg/L.min$), while the adsorbate equation for EB is $Kdye$ = 0.0184 L/mg.R is 0.9788, the estimated regression value, showing that the Langmuir-Hinshelwood kinetic model best describes the photodegradation of EB catalyzedby$g - C_{3N_4}$.

Using$g - C_{3N_4}$, the rate equation for the photocatalytic degradation of EB is

$$r = \frac{0.01426*[C_{dyw}]}{1+0.0184*[C_{dye}]} \qquad (7)$$

4. Conclusions

It was found that when $g - C_3N_4$ was exposed to ultraviolet (UV) rays, it performed admirably as a photocatalyst for the degradation of EB and MEO dye. This discovery was made possible by the fact that $g - C_3N_4$was produced as a by-product of the thermal decomposition of mylamine. The Langmuir-Hinshelwood model explained the process rather well. Which turned out to have pseudo-first-order kinetics after it was revealed to have such kinetics. The contact response time variable for MEO was determined to be 10.537 (mg/L.min), while the optimum value for Langmuir-Hinshelwood adsorbed was calculated to be 0.004 L/mg. For MB however, these numbers were determined to be 0.7756 (mg/L.min) and 0.0184 L/mg combined. The proportion of the dye, the amount of catalyst, and the pH were some of the operational factors that were observed to influence the rate of MEO and EB degradation. It was discovered that the ideal conditions for the photodegradation of MEO were 0.04 g/L catalyst in a solution with a pH of 7, whereas the optimal conditions for the photodegradation of EB were 0.08 g/L catalyst in a solution with a pH of 9.

References

[1] K.S. Meena, and K. Meena, Photocatalytic Decolorization of Textile dye Methylene blue by photocatalyst WO3 and SnO2. *Research Journal of Chemical Sciences ISSN*, *2231*:p.606X.

[2] S. Landi Jr, J. Carneiro, O.S. Soares, M.F. Pereira, A.C. Gomes, A. Ribeiro, A.M. Fonseca, P. Parpot,

and I.C. Neves, (2019). Photocatalytic performance of N-doped TiO2nano-SiO2-HY nanocomposites immobilized over cotton fabrics. *Journal of Materials Research and Technology*, *8*(2):pp.1933-1943.

[3] S.A.D. Ferreira, J.F. Donadia, G.R. Gonçalves, A.L. Teixeira, M.B.J.G. Freitas, A.A.R.Fernandes, and M.F.F. Lelis, (2019). Photocatalytic performance of granite waste in the decolorization and degradation of Reactive Orange 122. *Journal of Environmental Chemical Engineering*, *7*(3):p.103144.

[4] M.E. Ossman, and M.A. Fattah, (2015). Decolorization of textile effluent by photo catalytic degradation. *International Journal of Chemical and Biochemical Sciences*, *7*:pp.1-8.

[5] P. Jain, A. Kumar, N.Verma, and R.K. Gupta, R.K., (2019). In-situ synthesis of TiO2 nanoparticles in ACF: Photocatalytic degradation under continuous flow. *Solar Energy*, *189*:pp.35-44.

[6] A.J. Dos Santos, L.M.B. Batista, C.A.Martínez-Huitle, A.P.D.M Alves, and S. Garcia-Segura, (2019). Niobium oxide catalysts as emerging material for textile wastewater reuse: photocatalytic decolorization of azo dyes. *Catalysts*, *9*(12):p.1070.

[7] R. Shan, L. Lu, J. Gu, Y. Zhang, H. Yuan, Y. Chen, and B. Luo, (2020). Photocatalytic degradation of methyl orange by Ag/TiO2/biochar composite catalysts in aqueous solutions. *Materials Science in Semiconductor Processing*, *114*:p.105088.

[8] M.E. El-Naggar, A.R.Wassel, and K. Shoueir, (2021). Visible-light driven photocatalytic effectiveness for solid-state synthesis of ZnO/natural clay/TiO2 nanoarchitectures towards complete decolorization of methylene blue from aqueous solution. *Environmental Nanotechnology, Monitoring & Management*, *15*:p.100425.

[9] J. Schneider, M. Matsuoka, M. Takeuchi, J. Zhang, Y. Horiuchi, M.Anpo, and D.W. Bahnemann, (2014). Understanding TiO2 photocatalysis: mechanisms and materials. *Chemical reviews*, *114*(19):pp.9919-9986.

[10] A. Bhati, S.R. Anand, D. Saini, and S.K. Sonkar, (2019). Sunlight-induced photoreduction of Cr (VI) to Cr (III) in wastewater by nitrogen-phosphorus-doped carbon dots. *npj Clean Water*, *2*(1):p.12.

[11] L.A. Chanu, W.J. Singh, K.J. Singh, and K.N. Devi, (2019). Effect of operational parameters on the photocatalytic degradation of Methylene blue dye solution using manganese doped ZnO nanoparticles. *Results in Physics*, *12*:pp.1230-1237.

[12] S. Rajagopal, B.Paramasivam, and K.Muniyasamy, (2020). Photocatalytic removal of cationic and anionic dyes in the textile wastewater by H2O2 assisted TiO2 and micro-cellulose composites. *Separation and Purification Technology*, *252*:p.117444.

[13] S. Merouani, O. Hamdaoui, F.Saoudi, and M. Chiha, (2010). Sonochemical degradation of Rhodamine B in aqueous phase: effects of additives. *Chemical Engineering Journal*, *158*(3):pp.550-557.

[14] M.S.H. Bhuiyan, M.Y. Miah, S.C. Paul, T.D. Aka, O.Saha, M.M.Rahaman, M.J.I. Sharif, O.Habiba, and M. Ashaduzzaman, (2020). Green synthesis of iron oxide nanoparticle using Carica papaya leaf extract: application for photocatalytic degradation of remazol yellow RR dye and antibacterial activity. *Heliyon*, *6*(8):p.e04603.

[15] D.M. EL-Mekkawi, N.A.Abdelwahab, W.A. Mohamed, N.A.Taha, and M.S.A. Abdel-Mottaleb, (2020). Solar photocatalytic treatment of industrial wastewater utilizing recycled polymeric disposals as TiO2 supports. *Journal of cleaner production*, *249*:p.119430.